

# Quadrupole deformation in $\Lambda$ -hypernuclei

Bipasha Bhowmick <sup>a</sup>, Abhijit Bhattacharyya <sup>b</sup>, and G. Gangopadhyay <sup>c</sup>

Department of Physics, University of Calcutta  
92, Acharya Prafulla Chandra Road, Kolkata-700 009, India

the date of receipt and acceptance should be inserted later

**Abstract.** Shapes of light normal nuclei and  $\Lambda$ -hypernuclei are investigated using relativistic mean field approach. The FSUGold parametrization is used for this purpose. The addition of a  $\Lambda$  is found to change the shape of the energy surface towards positive deformation *i.e.* prolate shape. The deformation in a  $\Lambda$ -hypernucleus, when the hyperon is in the first excited state, is also discussed. The effect of the inclusion of the hyperon on the nuclear radius is generally small with one exception.

**PACS.** 21.80.+a Hypernuclei

## 1 Introduction

One of the unique and interesting aspects of hypernuclei is the structural change caused by the hyperon. As an impurity in normal nuclei, a hyperon may be expected to induce many effects on the core nucleus, such as change in size[1, 2], shape change, modification of its cluster structure[3], occurrence of nucleon and hyperon skin or halo[3, 4], shift of neutron drip line to more neutron-rich side[4, 5, 6] etc. Motoba *et al.*[7, 8] analyzed the light p-shell hypernuclei in the microscopic cluster model and studied the binding energy of ground state, excited states and transition probabilities. Owing to recent experimental developments some of those have been observed in light p-shell hypernuclei. As examples, we can refer to the reduction of  $B(E2)$  in  ${}^7_\Lambda\text{Li}$ [2] and the identification of the super-symmetric hypernuclear state in  ${}^9_\Lambda\text{Be}$ [9]. We can expect that a new experimental facility of Japan Proton Accelerator Research Complex (J-PARC) will reveal new spectral information on p and sd shell as well as neutron-rich hypernuclei.

As the shape of nuclei plays a decisive role in determining their properties, such as quadrupole moments and radii, mean field calculations have been performed in recent years to investigate the change of nuclear shape due to the addition of a  $\Lambda$  hyperon. Deformed Skyrme-Hartree-Fock(SkHF) studies in Ref. [10] have shown that the deformation of any hypernucleus is slightly less than the corresponding core nucleus. On the other hand, relativistic mean field (RMF) study in Ref. [11] found that the deformation completely disappears in  ${}^{13}_\Lambda\text{C}$  and  ${}^{29}_\Lambda\text{Si}$  hypernuclei though the corresponding normal core nuclei are deformed. Recently, a study with anti-symmetrized molec-

ular dynamics by Isaka *et al.*[12] have found that the  $\Lambda$  in p-wave enhances the nuclear deformation, while that in s-wave reduces it.

To perform a systematic and quantitative study of the structure change of the p and sd-shell nuclei, caused by the hyperon, we study the binding energy, quadrupole deformation, and the root mean square radii of a number of hypernuclei within a RMF model. The relativistic mean field theory of nucleus has been fairly successful in reproducing the properties of finite nuclear systems[13]. It has also been extensively applied to the study of hypernuclei[14].

## 2 Model Calculation

There have been a number of RMF parametrizations for prediction of the nuclear ground state properties. In the present work the FSUGold Lagrangian density has been employed[15]. This parametrization has already been extended to include hyperons and to study the properties of hypernuclear systems[16]. In this work it is used to study the change in quadrupole deformation due to addition of hyperon.

The parameters of the  $\Lambda N$  interaction have been determined by fitting the experimental separation energies of 12 hypernuclei in the mass region 16 to 208[16]. The masses of the two physical mesons have been taken from experiment. The nucleon mass is taken as 939 MeV. The mass of the  $\Lambda$  has been fixed at 1115.6 MeV.

In the present work, we have chosen to limit the type of deformation to azimuthally symmetric and reflection symmetric systems which corresponds to prolate and oblate ellipsoids for quadrupole deformation. This eliminates all the three-vector components of the boson fields. Therefore, the limitation on the type of deformation simplifies the calculation with contributions from only the scalar

<sup>a</sup> bips.gini@gmail.com

<sup>b</sup> abphy@caluniv.ac.in

<sup>c</sup> ggphy@caluniv.ac.in

meson, the zero components of the isoscalar vector meson, the photon, and the neutral  $\rho$  meson fields. This is the same set of boson fields that was required for spherical nuclei; however, these boson fields now have an additional angular dependence.

Solving the field equations with no further simplification can be very involved due to the difficulties encountered in obtaining solutions for coupled partial differential equations. We expand the boson fields in terms of Legendre polynomials and the nucleonic orbital wave functions in terms of spherical angle functions. The method of solution has been explained in detail in Ref. [17]. Terms up to angular momentum  $L = 6$  have been taken into account. The grid size for solving the differential equations is taken to be 0.1 fm.

Using density functional theory, H  kkinen *et al.*[18] showed that light nuclei and clusters of alkali-metal atoms have similar shapes and odd-even staggering of total energy, which they found to be nearly independent of the interactions between the fermions. In very light nuclei, the spacings between energy levels are large. Hence, pairing is not expected to play a very important role. In a deformed RMF calculation, Arumugam *et al.*[19] found that pairing is unimportant in light nuclei. Hence, in the present calculation, we have neglected pairing. In the case of  ${}_{\Lambda}^{25}\text{Mg}$ , we have checked that the deformation becomes slightly smaller in both the core and the hypernucleus on inclusion of the pairing. However, the relative change in deformation on inclusion of the hyperon is unaffected by pairing.

As will be seen, it has been necessary to study the energy surface of the ground state as a function of quadrupole deformation. To calculate the energy surface as a function of quadrupole deformation, we have used the method of Lagrange's undetermined multiplier. Thus the deformation constrained Lagrangian density has been written as

$$\mathcal{L}' = \mathcal{L} - \lambda \hat{Q}_D \bar{\Psi} \Psi, \quad (1)$$

where  $\hat{Q}_D = f(r)(3z^2 - r^2)$  is the quadrupole operator multiplied by a radial damping function  $f(r)$ . Lagrange's equations have been obtained from eqn. (1) and numerical solutions have been obtained for them. Following the method outlined in [20], the value of  $\lambda$  has been adjusted to obtain the given expectation value of  $\hat{Q}_D$ . Bassichis *et al.*[20] have shown that the lowest energy solution is obtained for each  $\langle \hat{Q}_D \rangle$ . For each  $Q_D$ , we have calculated the quadrupole deformation parameter  $\beta$  from the charge quadrupole moment using the relation

$$Q_p = \sqrt{\frac{16\pi}{5}} \frac{3}{4\pi} Z R_0^2 \beta \quad (2)$$

where  $R_0 = 1.2A^{1/3}$  fm.

The proton root mean square (rms) radius is defined as

$$r_p = \sqrt{\frac{1}{Z} \int r^2 \rho_p d\mathbf{r}} \quad (3)$$

Here  $\rho_p$  denotes proton density. Neutron rms radius ( $r_n$ ) and nuclear rms radius ( $r$ ) are also calculated in an analogous way. The nuclear radius, in case of hypernuclei, includes the effect of the hyperon also in the sense that the density in the above equation includes proton, neutron and hyperon densities.

### 3 Results

We calculate the quadrupole deformation parameter and the rms radii for a number of  $\Lambda$ -hypernuclei up to  $A < 30$  putting the  $\Lambda$  in its deformed ground state and also in the first excited state, which have opposite parities. The results of our calculation are presented in Table 1.

In our calculation, the ground state of  $\Lambda$  is a pure  $s$ -state as the higher positive parity states are too high in the continuum. The first excited state is a negative parity state which has contributions from both the  $p$  orbitals. We thus indicate the solutions for hypernuclei with the hyperon in the ground or the first excited states with 's' and 'p' in parentheses in the table and in the relevant figures. We have looked for both prolate as well as oblate minima in normal nuclei and hypernuclei. It is observed that in all the cases, the deformed hypernuclear minimum corresponds only to prolate deformation. The lowest state in the  $p$ -shell, the  $p_{1/2}$  state, splits up in  $K^\pi = 1/2^-$  and  $K^\pi = 3/2^-$  Nilsson states in presence of reflection symmetric axial deformation. For positive deformation, the former is the lowest energy state. Thus, in case of the excited state, the hyperon occupies the  $K^\pi = 1/2^-$  state. No oblate minima are observed in the hypernuclear systems. This observation will be elaborated later in this work. Very little information is available for the  $\Lambda$  separation energy in the ground state of the hypernucleus; the existing experimental values agree reasonably well with our calculation.

From Table 1, we see that when the  $\Lambda$  is placed in the ground state, the deformation changes slightly on inclusion of the hyperon, with only one exception in the case of  ${}_{\Lambda}^{13}\text{C}$ . The ground state of the core nucleus is generally prolate, with the exception of  ${}^{12}\text{C}$  and  ${}^{28}\text{Si}$ , the former of the two being oblate and the latter spherical. Except in these two nuclei, the deformation, on inclusion of a hyperon in the lowest energy state, may increase as well as decrease, but in general the shape remains similar to that of the core nucleus in its ground state.

However, in the case of  ${}_{\Lambda}^{13}\text{C}$ , the shape appears to change drastically on the inclusion of the  $\Lambda$ . The ground state of  ${}^{12}\text{C}$  shows negative deformation *i.e.* oblate shape, whereas the corresponding hypernucleus  ${}_{\Lambda}^{13}\text{C}$  is prolate. This is consistent with the fact that the energy surface plotted against quadrupole deformation (Fig. 1) shows an oblate minimum in the core nuclei but not in the hypernuclei.

This necessitated further investigation where we study the total energy of the system against deformation in a constrained calculation. In Fig. 1 we have represented the total binding energy with respect to the minimum ( $E_{tot}$ -

**Table 1.** Calculated Binding energy/nucleon ( $-E/A$ ) and  $\Lambda$  separation energy ( $E_\Lambda$ ) in MeV, quadrupole deformation parameter  $\beta$ , and the rms radius in fm at the minimum energy for the core nucleus and the corresponding hypernucleus in different  $\Lambda$  states.

Nucleus ( $\Lambda$ -state)	$-E/A$	$E_\Lambda$	$\beta$	$r_p$	$r_n$	$r$
$^8\text{Be}$	5.668	-	0.38	2.41	2.31	2.36
	5.533		-0.37	2.39	2.28	2.33
$^9_\Lambda\text{Be}$ (s)	5.837	7.189*	0.34	2.40	2.38	2.34
$^{10}\text{B}$	6.201	-	0.27	2.41	2.26	2.33
	6.116		-0.20	2.39	2.24	2.32
$^{11}_\Lambda\text{B}$ (s)	6.501	9.501	0.33	2.54	2.34	2.40
$^{12}\text{C}$	7.175	-	-0.21	2.36	2.18	2.27
$^{13}_\Lambda\text{C}$ (s)	7.534	11.842†	0.13	2.59	2.20	2.39
$^{13}_\Lambda\text{C}$ (p)	6.683	0.779	0.14	2.61	3.00	2.92
$^{18}\text{F}$	7.562	-	0.14	2.70	2.45	2.58
	7.561		-0.11	2.69	2.44	2.57
$^{19}_\Lambda\text{F}$ (s)	7.883	13.661	0.13	2.71	2.52	2.56
$^{19}_\Lambda\text{F}$ (p)	7.399	4.465	0.14	2.71	2.62	2.63
$^{22}\text{Na}$	7.565	-	0.22	2.85	2.57	2.72
	7.475		-0.13	2.83	2.55	2.69
$^{23}_\Lambda\text{Na}$ (s)	7.904	15.362	0.21	2.86	2.62	2.70
$^{23}_\Lambda\text{Na}$ (p)	7.537	6.921	0.22	2.86	2.69	2.74
$^{24}\text{Mg}$	7.814	-	0.25	2.91	2.60	2.76
	7.640		-0.15	2.89	2.59	2.74
$^{25}_\Lambda\text{Mg}$ (s)	8.142	16.014	0.23	2.91	2.65	2.74
$^{25}_\Lambda\text{Mg}$ (p)	7.823	8.039	0.24	2.91	2.71	2.78
$^{25}\text{Mg}$	7.872	-	0.20	2.88	2.64	2.76
	7.793		-0.13	2.87	2.63	2.75
$^{26}_\Lambda\text{Mg}$ (s)	8.248	17.648	0.22	2.92	2.63	2.75
$^{26}_\Lambda\text{Mg}$ (p)	7.927	9.30	0.23	2.92	2.69	2.79
$^{25}\text{Al}$	7.657	-	0.15	2.95	2.56	2.77
	7.565		-0.11	2.94	2.55	2.76
$^{26}_\Lambda\text{Al}$ (s)	8.001	16.601	0.14	2.95	2.61	2.75
$^{26}_\Lambda\text{Al}$ (p)	7.676	12.103	0.15	2.95	2.67	2.79
$^{26}\text{Al}$	7.828	-	0.11	2.92	2.60	2.76
	7.795		-0.09	2.92	2.59	2.76
$^{27}_\Lambda\text{Al}$ (s)	8.200	17.872	0.13	2.96	2.59	2.76
$^{27}_\Lambda\text{Al}$ (p)	7.874	9.07	0.14	2.96	2.65	2.80
$^{28}\text{Si}$	8.080	-	0.00	2.95	2.54	2.77
$^{29}_\Lambda\text{Si}$ (s)	8.453	18.897	0.06	3.00	2.54	2.78
$^{29}_\Lambda\text{Si}$ (p)	8.118	9.182	0.06	3.00	2.60	2.82

\*Exp. value is  $6.71 \pm 0.04$  MeV[21]

†Exp. value is  $11.69 \pm 0.12$  MeV[21]

$E_{\text{tot}}^{\text{min}}$ ) for  $^{12}\text{C}$  and  $^{13}_\Lambda\text{C}$  as a function of deformation parameter  $\beta$ . We see that the energy surface of  $^{12}\text{C}$  is almost flat with a oblate minimum around  $\beta = -0.2$ . Though there is no minimum for positive deformation, around  $\beta = 0.1$  there exists a region which might have formed a minimum. Inclusion of the  $\Lambda$  makes the oblate minimum disappear and the prolate minimum is found to be formed in the energy surface of  $^{13}_\Lambda\text{C}$ . One can see that although the unconstrained calculations predict the ground state of  $^{12}\text{C}$  and  $^{13}_\Lambda\text{C}$  to be oblate and prolate, respectively, actually a flat minimum is being replaced by a sharper prolate one. Our result is different from the previous HF calculations by

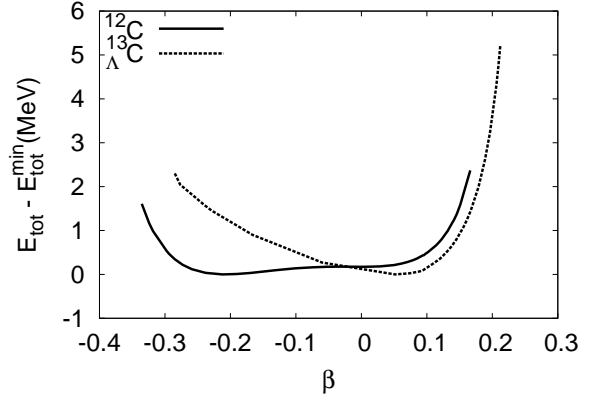


**Fig. 1.** Total energy with respect to the minimum ( $E_{\text{tot}} - E_{\text{tot}}^{\text{min}}$ ) as function of deformation  $\beta$  for  $^{12}\text{C}$  and the corresponding hypernucleus  $^{13}_\Lambda\text{C}$ .

Zhou *et al.*[10] or the SkHF+BCS calculations by Win *et al.*[22], which have reported similar deformations for  $^{12}\text{C}$  and  $^{13}_\Lambda\text{C}$ . Some calculations have also reported a spherical configuration for  $^{13}_\Lambda\text{C}$ [11,12,23].

As a case where deformation appears in hypernuclei while the core is spherical in our calculation, we study  $^{29}_\Lambda\text{Si}$ . However, we should point out that  $^{28}\text{Si}$  is experimentally known to be a deformed nucleus. We see that  $^{29}_\Lambda\text{Si}$  is slightly prolate with the FSUGold parameter whereas  $^{28}\text{Si}$  is spherical. In Fig. 2 we have represented the total binding energy with respect to the minimum ( $E_{\text{tot}} - E_{\text{tot}}^{\text{min}}$ ) for  $^{28}\text{Si}$  and  $^{29}_\Lambda\text{Si}$  as a function of deformation. From Fig. 2,

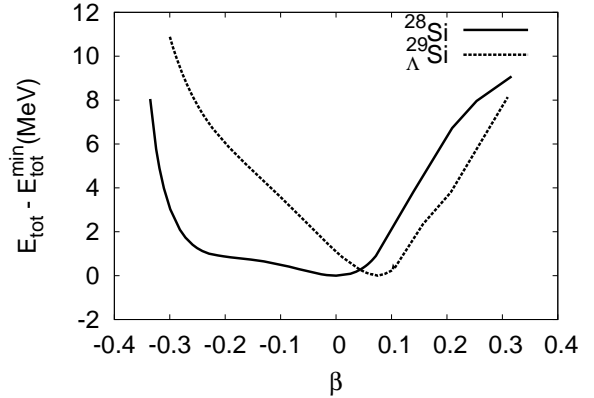


**Fig. 2.** Total energy with respect to the minimum as function of deformation  $\beta$  for  $^{28}\text{Si}$  and the corresponding hypernucleus  $^{29}_\Lambda\text{Si}$ .

we see that the rather flat energy minima at the spherical configuration in case of  $^{28}\text{Si}$ , becomes sharper and shifts slightly towards positive side in case of  $^{29}_\Lambda\text{Si}$ . One can also see that in the case of  $^{28}\text{Si}$ , a very slight change in the energy surface may make the ground state oblate consistent with the large deformation observed experimentally.

The situations in both the above cases may be considered as follows. The energy surfaces around the minima

are rather flat, irrespective of the actual positions of the minima. The  $1\Lambda s_{1/2}$  state, on the other hand, has a shallow prolate minimum. The reason for the minimum occurring only on the prolate side requires further analysis which we plan to carry out in a future work. The inclusion of the  $\Lambda$ -hyperon in the  $1s_{1/2}$  state is thus strong enough to polarize the core. Although individually the prolate minimum for the  $1\Lambda s_{1/2}$  state is not very deep, the interaction between the hyperon and the nucleons leads to a change in the energy levels of normal nucleons also, driving the nucleus towards positive deformation. Thus the overall surface shows a sharper prolate minimum. In case where the minimum is deep enough in the core nucleus, the hyperon does not change the shape. For example, the nucleus  $^{16}\text{O}$ , being doubly magic, is known to be spherical and has a deep minimum around  $\beta = 0$ . We find that the corresponding hypernucleus  $^{17}_{\Lambda}\text{O}$  is also spherical.

We also note that our results for  $^{25}_{\Lambda}\text{Mg}$  agree with the SkHF+BCS calculations by Win *et al.*[22] in the sense that inclusion of a hyperon decreases the total deformation slightly. However, our results, as a whole, are different from the previous RMF and SkHF calculations[4, 5, 10, 11, 22, 23] in the sense that all the previous calculations report a decrease in deformation on addition of a  $\Lambda$  particle. Our calculations show that the deformation may increase in some cases. In general, the inclusion of the  $\Lambda$  hyperon makes the energy surface sharper, the oblate minima disappears and the prolate one becomes prominent, thus producing a shift in deformation. Similar observations have been found for the other nuclei investigated in Table 1.

In the case of excited  $\Lambda$  states, our calculations show that when the  $\Lambda$  goes from the ground-state to the p-state it slightly increases the deformation excluding the case of  $^{29}_{\Lambda}\text{Si}$ , where the deformation remains the same. Calculation for the deformation of hypernuclei for an excited  $\Lambda$  state reported by Isaka *et al.*[12] found similar results. In  $^9_{\Lambda}\text{Be}$  and  $^{11}_{\Lambda}\text{B}$ , the excited  $\Lambda$  state is unbound.

We have also investigated the changes in the rms radii of the hypernuclei. Proton, neutron and total rms radii are shown in the last three columns of Table 1.

It is seen that the inclusion of a  $\Lambda$  hyperon, causes either a slight increase or no modification in neutron and proton radii when the  $\Lambda$  particle is in the s-state. When the hyperon is excited to the p-state the size of the hypernucleus increases only slightly in almost all cases. The only exception is  $^{13}_{\Lambda}\text{C}$ , where this increase in radius is significant, so that the hypernucleus is much larger than the corresponding core nucleus. The reason for this large increase is the change in shape. As already pointed out, the core in  $^{13}_{\Lambda}\text{C}$  is an oblate spheroid while the hypernucleus is prolate. The hypernucleus being elongated along the symmetry axis shows a larger radius.

We should point out that in contrast to many calculations, we have not obtained any shrinkage in the ground state of the hypernucleus. We have already discussed the case of  $^{13}_{\Lambda}\text{C}$ . In  $^{11}_{\Lambda}\text{B}$  and  $^{29}_{\Lambda}\text{Si}$ , where the positive deformation has increased, we find a more significant increase in proton radius. Otherwise the proton radius is nearly equal to that of the core nucleus. In almost no case we have

got a shrinkage. The neutron radius increases in almost all cases. A recent RMF calculation have also found no change in proton radius[24] though it should be added that the hypernuclei studied in that work are beyond the mass range of the present work. The experimental evidence of shrinkage in charge radius is the decrease in  $B(E2)$  in  $^7_{\Lambda}\text{Li}$ , a very light nuclei observed by Tanida *et al.*[2]. In our case, we get a slight decrease in the lightest nuclei,  $^9_{\Lambda}\text{Be}$ .

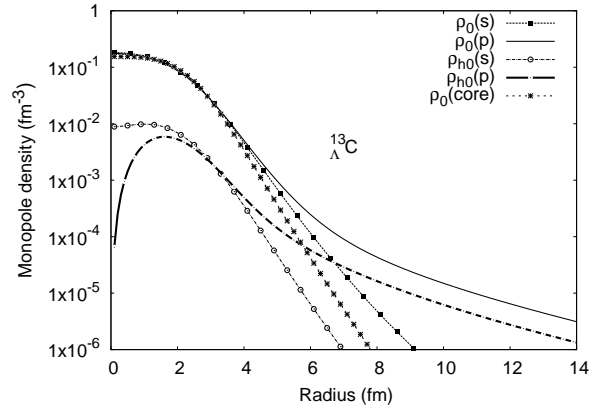


**Fig. 3.** The monopole nucleon and hyperon density profile in  $^{13}_{\Lambda}\text{C}$  when the  $\Lambda$  is in different single particle state (s and p, given in parentheses). Here  $\rho_o$  refer to monopole nucleon density and  $\rho_{h0}$  refer to monopole hyperon density. The density of the core nucleus  $^{12}\text{C}$  ( $\rho_0(\text{core})$ ) is also shown. .

The reason for the large increase in size in  $^{13}_{\Lambda}\text{C}$  can be seen in the distribution of densities of the nuclei. We plot the monopole densities in  $^{13}_{\Lambda}\text{C}$  and  $^{25}_{\Lambda}\text{Mg}$  in Figs. 3 and 4, respectively, to see the effect of the hyperon. Both the cases with the hyperon in its ground state and excited state are shown. In Fig. 3, the monopole density of  $^{12}\text{C}$  is also shown. One can see that the density profile of this core nucleus differs from that of the normal nucleons in  $^{13}_{\Lambda}\text{C}$ , an evidence of the change in the ground state as discussed earlier.

Fig. 3 shows that in  $^{13}_{\Lambda}\text{C}$ , when the hyperon is placed in the p-state, the densities extend to larger distances. Actually, the hyperon is very loosely bound in the excited state. Hence, its wave function extends to a very large distance. As the hyperon interacts strongly with the nucleons, the nucleon density also shows a large tail, reminiscent of halo nuclei.

However, this is not a general phenomenon as evident from Table I. As an example, we present the density profile for  $^{25}_{\Lambda}\text{Mg}$  in Fig. 4. It is clear that in this hypernucleus, both the nucleon and the hyperon densities remain practically unchanged whether the hyperon is in the s-state or in the p-state. The p-shell hyperon in this case is strongly bound and does not show any halo-like behaviour.

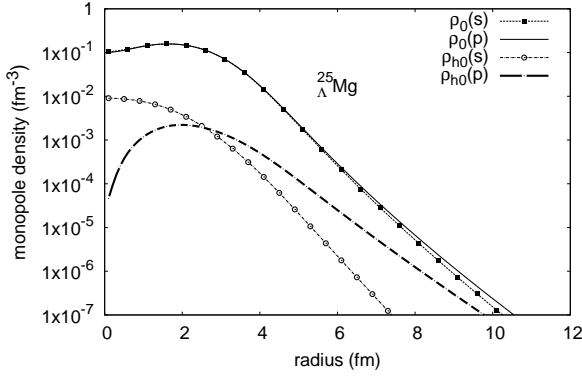


**Fig. 4.** The monopole nucleon and hyperon density profile in  $^{25}_{\Lambda}\text{Mg}$  when the  $\Lambda$  is in different single particle state (s and p). See caption of Fig. 3 for details.

## 4 Summary

We have studied the deformation of core and hypernuclei in the RMF approach using the FSUGold parameter set. The calculated  $\Lambda$  binding energies agree reasonably well with the experimentally observed values. We see that the inclusion of a  $\Lambda$  hyperon changes the energy surface making it steeper. There exists no oblate minimum in any light hypernucleus. Results of the present calculation differ from the previous ones. The latter usually predict that inclusion of a  $\Lambda$  tends to drive the shape to spherical. Our results show that the change in  $\beta$  is usually small with possible exceptions. If the core nucleus is prolate, the deformation may increase in some cases on addition of a hyperon. In general, the nucleon density profile changes to a small extent on inclusion of the hyperon, whether in the ground state or the first excited state. When the  $\Lambda$  goes to the p-state, both the deformation and radius increases by a small amount. The only exception is  $^{13}_{\Lambda}\text{C}$  where, the hyperon being very loosely bound, creates a halo-like structure.

This work was carried out with financial assistance of the UGC (UPE, RFSMS, DRS) and DST of the Government of India.

## References

1. E. Hiyama, M. Kamimura, K. Miyazaki, T. Motoba, Phys. Rev. C **59**, 2351 (1999).
2. K. Tanida et al., Phys. Rev. Lett. **86**, 1982 (2001).
3. E. Hiyama, M. Kamimura, T. Motoba, T. Yamada, Y. Yamamoto, Phys. Rev. C **53**, 2075 (1996).
4. H. F. Lu, J. Meng, S. Q. Zhang, S. G. Zhou, Eur. Phys. J. A **17**, 19 (2003).
5. X.-R. Zhou, A. Polls, H.-J. Schulze, I. Vidana, Phys. Rev. C **78**, 054306 (2008).
6. B. Bhowmick, A. Bhattacharyya, G. Gangopadhyay, Int. J. Mod. Phys. E **22**, 1350012 (2013).
7. T. Motoba, H. Bando, K. Ikeda, Prog. Theor. Phys. **70**, 189 (1983); **71**, 222 (1984).
8. T. Motoba, H. Bando, K. Ikeda, T. Yamada, Prog. Theor. Phys. Suppl. **81**, Chap. 3 (1985).
9. O. Hashimoto, H. Tamura, Prog. Part. Nucl. Phys. **57**, 564 (2006), and references therein.
10. X.R. Zhou, H.-J. Schulze, H. Sagawa, C.X. Wu, E.G. Zhao, Phys. Rev. C **76**, 034312 (2007).
11. M. T. Win, K. Hagino, Phys. Rev. C **78**, 054311 (2008).
12. M. Isaka, M. Kimura, A. Dote, A. Ohnishi, Phys. Rev. C **83**, 044323 (2011).
13. P. Ring, Prog. Part. Nucl. Phys. **37**, 193 (1996).
14. H. Shen, F. Yang, H. Toki, Prog. Theor. Phys. **115**, 325 (2006) and references therein.
15. B.G. Todd-Rutel, J. Piekarewicz, Phys. Rev. Lett. **95**, 122501 (1995).
16. B. Bhowmick, A. Bhattacharyya, G. Gangopadhyay, Int. Jour. Mod. Phys. E **21**, 1250069 (2012).
17. G. Gangopadhyay, Phys. Rev. C **59**, 2541 (1999).
18. H. Håkkinen, J. Kolehmainen, M. Koskinen, P. O. Lipas, M. Manninen, Phys. Rev. Lett. **78**, 1034 (1997).
19. P. Arumugam, T.K. Jha, S.K. Patra, arXiv:nucl-th/0311091.
20. W. H. Bassichis and L. Wilets, Phys. Rev. Lett. **27**, 1451 (1971).
21. M. Juric et al., Nucl. Phys. B **52**, 1 (1973).
22. M. T. Win, K. Hagino, T. Koike, Phys. Rev. C **83**, 014301 (2011).
23. B. Lu, E. Zhao, S. Zhou Phys. Rev. C **84**, 014328 (2011).
24. R. Xu, C. Wu and Z. Ren, J. Phys. G: Nucl. Part. Phys. **39**, 085107 (2012).